

<b>REPORT DOCUMENTATION PAGE</b>				<b>Form Approved OMB No. 0704-0188</b>	
<small>Public reporting burden for this collection of information is estimated to average 1 hour per response, including the time for reviewing instructions, searching data sources, gathering and maintaining the data needed, and completing and reviewing the collection of information. Send comments regarding this burden estimate or any other aspect of this collection of information, including suggestions for reducing this burden to Washington Headquarters Service, Directorate for Information Operations and Reports, 1215 Jefferson Davis Highway, Suite 1204, Arlington, VA 22202-4302, and to the Office of Management and Budget, Paperwork Reduction Project (0704-0188) Washington, DC 20503.</small>					
<b>PLEASE DO NOT RETURN YOUR FORM TO THE ABOVE ADDRESS.</b>					
<b>1. REPORT DATE</b> (DD-MM-YYYY) OCT 08		<b>2. REPORT TYPE</b> Conference Paper Postprint		<b>3. DATES COVERED</b> (From - To) May 05 - May 08	
<b>4. TITLE AND SUBTITLE</b> A PHOTONIC RECIRCULATING DELAY LINE FOR ANALOG-TO-DIGITAL CONVERSIONS AND OTHER APPLICATIONS				<b>5a. CONTRACT NUMBER</b> In House AWGDSN01	
				<b>5b. GRANT NUMBER</b> N/A	
				<b>5c. PROGRAM ELEMENT NUMBER</b> 62702F	
<b>6. AUTHOR(S)</b> Henry Zmuda, Michael Fanto, Thomas McEwen, Jared Pawloski, and Kristina Norelli				<b>5d. PROJECT NUMBER</b> AWGD	
				<b>5e. TASK NUMBER</b> SN	
				<b>5f. WORK UNIT NUMBER</b> 01	
<b>7. PERFORMING ORGANIZATION NAME(S) AND ADDRESS(ES)</b> AFRL/RYDP 25 Electronic Parkway Rome, NY 13441-4514				<b>8. PERFORMING ORGANIZATION REPORT NUMBER</b> N/A	
<b>9. SPONSORING/MONITORING AGENCY NAME(S) AND ADDRESS(ES)</b> AFRL/RYDP 25 Electronic Parkway Rome, NY 13441-4514				<b>10. SPONSOR/MONITOR'S ACRONYM(S)</b> N/A	
				<b>11. SPONSORING/MONITORING AGENCY REPORT NUMBER</b> AFRL-RY-RS-TP-2008-9	
<b>12. DISTRIBUTION AVAILABILITY STATEMENT</b> Approved for public release: Distribution unlimited PA# WPAFB-08-0725					
<b>13. SUPPLEMENTARY NOTES</b> Paper published in Proc. of SPIE Vol. 6975 69750F. This material is declared a work of the U.S. Government and is not subject to copyright protection in the United States.					
<b>14. ABSTRACT</b> Experimental results for a photonic recirculating delay line for high-speed, high-resolution Analog-to-Digital Converted (ADC) and other applications is presented. The approach modifies an analog fiber optic link with a recirculating optical loop as a means to store a time-limited microwave signal so that it may be digitized by using a slower, conventional electronic ADC. Detailed analytical analysis of the dynamic range and noise figure show that under appropriate conditions the microwave signal degradation is sufficiently small so as to allow the digitization of a multi-gigahertz signal with a resolution greater than 10 effective bits. Experimental results provided support the theory.					
<b>15. SUBJECT TERMS</b> Photonic Analog-to-Digital Conversion, Microwave Photonics, Optical Signal Processing.					
<b>16. SECURITY CLASSIFICATION OF:</b>			<b>17. LIMITATION OF ABSTRACT</b>  UU	<b>18. NUMBER OF PAGES</b>  11	<b>19a. NAME OF RESPONSIBLE PERSON</b> Michael Fanto
<b>a. REPORT</b> U	<b>b. ABSTRACT</b> U	<b>c. THIS PAGE</b> U			<b>19b. TELEPHONE NUMBER (Include area code)</b>

# A PHOTONIC RECIRCULATING DELAY LINE FOR ANALOG-TO-DIGITAL CONVERSION AND OTHER APPLICATIONS

**Henry Zmuda**

Department of Electrical and Computer Engineering  
University of Florida,  
Gainesville, Florida

**Michael Fanto and Thomas McEwen**

Air Force Research Laboratory Photonics Center  
Rome, NY

**Jared Pawloski**

Department of Electrical Engineering  
State University of New York, Binghamton, NY

**Kristina Norelli**

Department of Biomedical Engineering  
Syracuse University, Syracuse, NY

## ABSTRACT

Experimental results for a photonic recirculating delay line for high-speed, high-resolution Analog-to-Digital Converter (ADC) and other applications is presented. The approach modifies an analog fiber optic link with a recirculating optical loop as a means to store a time-limited microwave signal so that it may be digitized by using a slower, conventional electronic ADC. Detailed analytical analysis of the dynamic range and noise figure shows that under appropriate conditions the microwave signal degradation is sufficiently small so as to allow the digitization of a multi-gigahertz signal with a resolution greater than 10 effective bits. Experimental results provided support the theory.

**Keywords:** Photonic Analog-to-Digital Conversion, Microwave Photonics, Optical Signal Processing.

## 1. INTRODUCTION

An analog-to-digital converter (ADC) is a key element linking the collection of analog sensor data and converting it to a binary representation suitable for digital processing. The realization of a high-speed, high-resolution ADC has proven itself a difficult task, and the potential for using optical processing as a means to achieve high-speed conversion has long intrigued system designers [1,2]. Although there has been significant progress with high-speed electronic ADC systems, the ability to achieve conversion rates (at least  $10^{10}$ -samples per second) at a reasonable resolution (greater than 4 - 6 bits) remains an elusive goal [3, 4].

Though a wide variety of approaches exist for the implementation of an all-photonic high speed ADC [5-10], much emphasis has been placed on taking full advantage of advances in electronic ADC technology [11-14]. The latter type of approach is generally termed an *optically assisted* ADC, and uses optical techniques to condition the high-speed signal to be digitized in such a way that a comparatively lower-speed electronic ADC can be used to perform the actual digitization. Such an approach is especially attractive in that it allows the optical ADC architecture to keep pace with

advances in electronic ADC technology. Specifically, as the speed and resolution of electronic ADC's continue improve, the optical portion of the system is used to further enhance the performance of the overall system.

This paper shows how a conventional analog fiber optic link can be augmented with a recirculating optical delay loop so as to realize an optically assisted ADC that provides improved performance in terms of both speed and resolution using one (slower) electronic ADC. The overall architecture is quite simple and readily integrates with any electronic ADC system. Moreover, the high-speed ADC performance is fundamentally limited by the performance of the fiber optic link. Since high fidelity fiber optic links, specifically links having a large dynamic range, are the subject of ongoing research, improved link performance will translate directly to improved ADC performance. The approach also has the distinct advantage in that it can be configured to provide both high-speed and high resolution thereby avoiding the speed-resolution tradeoffs that have plagued ADC system designers.

Section 2 of this paper explains the overall system operation, specifically the speed-resolution tradeoff, by quantifying how the recirculating delay loop degrades the fiber optic link performance, and finally Section 3 presents proof-of-principle experimental results.

## 2. SYSTEM OPERATION

### 2.1 Timing and Bandwidth Considerations

We assume that the sampling rate is determined from the Nyquist criteria, namely that an RF signal whose highest frequency component is  $f_{\max}$  requires a sampling rate of  $s_f$  samples per second, corresponding to a sampling interval of  $T_f$ , where  $T_f = s_f^{-1} = (2f_{\max})^{-1}$ . A signal of duration of  $T$  seconds would require  $N = \text{integer}(T \cdot s_f)$  high-speed samples, while these same  $N$  sample values can be (ideally) captured from the periodic extension of the time-limited RF input. This in turn allows the input signal to be digitized using a (comparatively slow) ADC, sampling at a reduced rate with associated sampling interval  $T_s$ , where  $T_s = T + T_f$ . Thus, successive *samples* of the high-speed signal can be acquired from properly timed successive *periods* of the input signal. It is seen then that the required  $N$  high-speed samples can be captured from  $N$  periods. The number of periods required to capture the necessary input information thus represents a fundamental parameter in the analysis to follow. Note however that the timing jitter requirements (aperture uncertainty) are the same as those for the high-speed ADC, an issue examined later in this paper. The time-limited requirement of the signal also provides a low frequency limit of  $f_{\min} = 2T_s^{-1}$ , though this is of lesser significance than maximum frequency, it does pose an engineering issue relating the maximum frequency, bandwidth, and number of samples that would need to be addressed for a given application.

### 2.2 Photonic System

A block diagram showing the details for modifying an analog fiber optic link with a recirculating (optical) delay line so as to produce the periodic extension of the microwave input signal as well as the associated low-speed ADC is shown in Figure (1). Referring to Figure (1), the signal to be digitized first amplitude modulates a CW laser. The signal conditioning shown provides for sign-bit extraction and any amplification, level shifting, or band limiting that may be required for optimal link performance. Such signal preconditioning is present in any ADC and is not considered further in this paper. For proper operation of the system it is imperative that the RF input signal be strictly time-limited, and this can be accomplished in a number of ways. Figure (1) shows an optical switch (OS) at the output of the modulator. This switching operation can be realized in the optical domain, for example, with a high-speed electrooptic or acoustooptic switch or an electroabsorption modulator that interrupts the optical path after the required length of time. Alternatively, the time-limiting operation can be performed electronically at the input to the amplitude modulator. This optically modulated, time limited RF signal is then injected into the recirculating loop by means of an optical coupler. The purpose of the recirculating delay (with a loop transit time of  $T$  seconds) is to produce the (nominally) periodic replicas of the input signal of period  $T$  as discussed. The recirculating loop contains a semiconductor optical amplifier (SOA) to compensate for any losses in the loop and an isolator to insure one-way loop circulation. An appropriate length of optical

fiber is used to (roughly) establish the necessary time delay  $T$  while a variable delay line trimmer is included to precisely adjust the loop delay to the exact value. This required loop length can be computed, assuming that the signal essentially propagates in optical fiber as  $n_f L = c T_s$  where  $c$  is the speed of light in free space and  $n_f$  is the fiber group index. To prevent time-aliasing as the optically modulated RF signal recirculates, a second time limiting optical switch is also included in the delay loop as a means to purge the recirculating signal once the digitalization process is completed so that the operation may start again with the next input signal packet to be digitized. If the gain of the SOA were adjusted to exactly compensate for the loss, the system would essentially act as a ring cavity laser resonating at frequencies where the loop phase-shift is an integer multiple of  $2\pi$ . Since the loop time delay is relatively long, perhaps as long as several microseconds, the loop will support a very large number of resonances. With the lack of any frequency selective device in the loop, lasing at any particular wavelength(s) is not likely. Under proper operating conditions, the coherent addition of the optically-modulated RF signal will never occur in the loop. This suggests that is necessary, a polarization scrambler can be included in the loop, resulting in a polarization dependent loss that is not compensated by the SOA gain and hence completely suppress any laser oscillations. Upon exiting the loop via the input/output coupler, the delayed, RF modulated optical signal is detected and demodulated by a high-speed photodetector. Note also that the first pulse to exit the system will not have traversed the recirculating delay loop but rather passes directly through the input/output coupler. Because of the possible disparity in amplitude level this pulse may not be directly usable as part of the signal to be digitized. It can however be useful as a header signal indicating to the electronic ADC system that an input signal is forthcoming. Once again, if necessary, the detected electrical signal may be appropriately conditioned before being digitized by the low-speed ADC.

As Figure (1) suggests, with the exception of the recirculating delay loop, the remaining components consist simply of a conventional fiber optic link. Clearly then the performance of the complete system will be ultimately limited by the performance of the fiber link used. The analysis to follow will thus concentrate on how the inclusion of the recirculating delay line degrades the performance of this fiber link. Once this degradation has been quantified, the link specification needed to meet an overall ADC performance requirement can be stated.

Proper evaluation of the performance of the ADC system requires that several factors be quantified. These include the exact nature of the loop timing, the degradation in the dynamic range of the RF input signal with each loop circulation, the restrictions on the input signal-to-noise ratio (SNR) so as to achieve a specified effective number of bits for the ADC, and timing jitter (aperture uncertainty), and these factors are now examined.

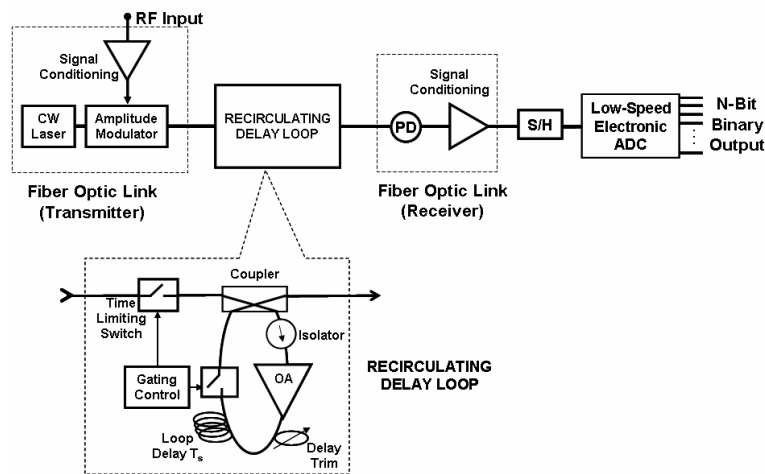


Figure 1: Block diagram of the modification of a fiber optic link with a recirculating delay line to realize an optically assisted ADC.

### 2.3 Noise Figure, Signal-to-Noise Ratio, and Effective Number of Bits

In addition to the ADC conversion speed, another major factor limiting the ADC performance is the effective number of bits (ENOB). This is generally expressed in terms of the dynamic range of the overall system. For a broadband fiber optic link, the dynamic range is limited by intermodulation products introduced by the modulator nonlinearities. The maximum allowable RF input signal that can be applied to the modulator occurs when the power contained in the first intermodulation product at the output just equals the power in the noise floor. This defines the spur-free dynamic range (SFDR) or the maximum SNR. The maximum allowable input voltage determines the full-scale voltage  $V_{FS}$ . For a B-bit ADC, the full-scale voltage is expressed as  $V_{FS} = 2^B V_{LSB}$ , where  $V_{LSB}$  is the minimum voltage (corresponding to the least significant bit) that can be resolved. For an arbitrary input signal, it is usual to assume that the signal quantization error is uniformly distributed over the sampling interval which results in an rms noise voltage of  $V_{noise_{rms}} = \frac{V_{LSB}}{\sqrt{12}}$  [3].

The ratio of the rms value of the full-scale voltage to  $V_{noise_{rms}}$  gives the classical result relating the SNR and resolution (ENOB)  $B$ , namely

$$SNR = \frac{3}{2} 2^{2B} \quad (1)$$

Equation (1) establishes the ENOB available from an ADC due to the SNR alone.

The inclusion of the recirculating loop will degrade the dynamic range of the link. The degradation in the SNR of the RF-input signal as it propagates through the recirculating delay loop the required  $N$  number of times is readily characterized by the overall system noise figure, defined as

$$F_{RF}(N) = \frac{SNR_{without\ recirculating\ loop}}{SNR_{with\ recirculating\ loop}} \Bigg|_{Same\ Gain} \quad (2)$$

assuming the same RF link gain for both cases.

Referring again to Figure 1, let  $L_I > 1$  denote the isolator loss,  $L_c > 1$  the coupling ratio (splitting and excess loss),  $L_t > 1$  is the corresponding coupler through insertion loss, and  $L_{ex} > 1$  the total excess loop loss arising from connector loss as well as any other losses present in the loop. Also denote the gain of the optical amplifier as  $G_{SOA}$  with corresponding noise figure  $F_{SOA}$ . A straightforward analysis shows that the loop noise figure is

$$F_{Loop} = L_I \left( F_{SOA} + \frac{L_{ex} L_t - 1}{G_{SOA}} \right) \quad (3)$$

As the RF modulated optical signal circulates around the loop, the signal-to-noise ratio degrades with each pass. For the  $N^{th}$  loop circulation the associated noise figure  $F_{Loop}^{(n)}$  is

$$F_{Loop}^{(N)} = F_{Loop} + \frac{F_{Loop} - 1}{G_{Loop}} + \frac{F_{Loop} - 1}{G_{Loop}^2} + \dots + \frac{F_{Loop} - 1}{G_{Loop}^{N-1}} = F_{Loop} + \frac{F_{Loop} - 1}{G_{Loop}^{N-1}} \frac{1 - G_{Loop}^{N-1}}{1 - G_{Loop}} \quad (4)$$

where the loop gain is

$$G_{Loop} = \frac{G_{SOA}}{L_I L_t L_{ex}} \quad (5)$$

where  $L_t = 1 - L_c$  is the coupler thru loss. Since the link output is to be the periodic extension of the input, the SOA gain is adjusted so that  $G_{Loop} = 1$  so that Equation (4) becomes

$$F_{Loop}^{(N)} = N(F_{Loop} - 1) + 1 \quad (6)$$

Equation (6) shows that although after many loop circulations the signal will be largely corrupted by noise, it is still reasonable to expect that for values of integer  $N$  sufficiently small, a signal with a reasonable SNR can still exist in the loop. It will be seen later that values significantly greater than  $N = 10$  are quite reasonable.

Note also that some additional degradation in SNR occurs due the initial and final coupling into and out of the loop. This overall (optical) noise figure  $F^{(N)}$  is given by (again for the case of unity loop gain)

$$F^{(N)} = \begin{cases} L_t, & N = 0 \\ L_c L_t \frac{G_{SOA} F_{SOA} - 1 + L_c L_{ex}}{G_{SOA}}, & N = 1 \\ L_c \frac{G_{Loop}^{N+1} G_{SOA} F_N + G_{SOA} L_t F_{SOA} + L_t L_c L_{ex} - L_t - G_{SOA}}{G_{SOA} G_{Loop}}, & N > 1 \end{cases} \quad (7)$$

The SNR characteristics for direct-detection analog fiber optic link with external or direct modulation are well known [19]. The present discussion then serves only to indicate the manner by which the recirculating delay loop impacts the overall noise of the system. Three significant noise sources are present; input noise, detector noise (primarily shot, thermal, and dark current noise), and laser noise. The average noise power introduced in the detection process is designated,  $P_{Detector\ Noise}$  and is not effects by the presence of the recirculating loop. The average laser noise power, designated as  $P_{Laser\ Noise}$ , is primarily a result of the relative intensity noise ( $n_{RIN}$ ). Finally, the noise present at the modulator input, generally thermal noise, contributes a term  $P_{Input\ Noise}$ . The total electrical average noise power at the detector output can be expresses as

$$P_{Total\ Noise} = P_{Detector\ Noise} + G_{RF} P_{RF\ Input\ Noise} + F_o(0) n_{RIN} \quad (8)$$

where  $F_o(0)$  is the link noise figure in the absence of the recirculating loop and is given by

$$F_o = \frac{1 - \eta_{ex} + \eta_{ex} L_t}{\eta_{ex} \eta_{mod}} \quad (9)$$

and where the link RF gain is

$$G_{RF} = \frac{P_{out}}{P_{in}} = \left( \frac{\pi \rho \eta_{ex}^{-1} \cdot \eta_{mod}^{-1} \cdot G_N P_o |Z_{mod}|}{V_\pi} \right)^2 \frac{R_L}{R_{mod}} \quad (10)$$

In equation (10)  $\eta$  is the link gain/loss,  $P_o$  is the laser power,  $\rho$  is the detector responsivity,  $V_\pi$  represents the modulator extinction voltage,  $R_L$  is the load impedance, and  $Z_{mod}$  is the modulator input impedance with  $R_{mod} = \text{Re}\{Z_{mod}\}$

The major controllable factor influencing the total is due to the laser RIN, which can be minimized by using a solid-state laser. The system SNR can be further reduced using coherent detection but at the expense of a more complicated system.

From equation (2), the noise figure  $F(N)$  representing the degradation in SNR after  $N$  loop-circulations can be expressed,

$$F_{RF}(N) = \frac{SNR_{without\ loop}}{SNR_{with\ loop}} \Bigg|_{Same\ Link\ Gain} = \frac{n_d + G_{RF}n_{RF\ input} + F_o(N)n_{RIN}}{n_d + G_{RF}n_{RF\ input} + F_o(0)n_{RIN}} \quad (11)$$

where the noise figure with the recirculating loop present is given by

$$F_o(N) = \frac{1 - \eta_{ex} + \eta_{ex}L_t(L_t + F^{(N)} - 1)}{\eta_{ex}\eta_{mod}} \quad (12)$$

Equation (11) assumes  $G_{Loop} = 1$  and that the coupler ratio  $L_c$  is chosen to maintain the same link gain for no passes as for  $N$ -passes.

Since the SNR and link resolution  $B$  are related by equation (1), equation (11) allows the computation of the effective number of bits of the ADC as follows. Let  $B_o$  represent the link resolution without the recirculating loop and let  $B_{eff}$  be the resolution with the recirculating loop present. Then,

$$SNR_{with\ loop} = \frac{SNR_{without\ loop}}{F_{RF}(N)} = \frac{3}{2} \frac{2^{2B_o}}{F_{RF}(N)} = \frac{3}{2} 2^{2B_{eff}} \quad (13)$$

Solving for  $B_{eff}$  gives

$$B_{eff} = B_o - \frac{1}{2} \log_2 F_{RF}(N) \quad (14)$$

We see that the degradation in the SNR increases logarithmically with noise figure  $F(N)$ . With regard to the present system architecture the ADC performance can be captured effectively in terms of a reduction in the ENOB,  $B_r = B_o - B_{eff}$  or

$$B_r = \frac{1}{2} \log_2 F_{RF}(N) \quad (15)$$

To estimate expected performance, consider 3-dB couplers with a 1-dB insertion loss, and total excel loop loss of 3-dB, and an SOA with a 4-dB noise figure. From these, estimates for the corresponding noise figure as a function of the number of loop circulations can be obtained from Equation (11) and, more significantly, the reduction in the ENOB can be computed from Equation (15). For these estimates, the SOA gain was chose to exactly cancel the loop loss ( $\sim 4.5$  dB). This gives from Equation (3) a loop noise figure of just over 7.7 dB corresponding to a reduction in the ENOB. It is seen that even after several hundred-loop circulations the ENOB has been reduced by roughly four bits. This means that a link capable of resolving the desired number of bits plus the bit reduction is required. To place this in perspective, note that a 10 - bit ADC requires a Spur-Free Dynamic Range (SFDR) of roughly 60.4 dB. The present approach thus requires the ability to resolve 14-bits, or a SFDR of roughly 83.7 dB in a 5 GHz bandwidth for a 10 Gbps ADC. Expressed in terms if of a 1 Hz bandwidth, a SFDR of 148.3 dB is required. State-of-the-art broadband (18 GHz) analog fiber optic links have a SFDR in excess of 130 dB, hence, at the reduced bandwidth the link requirement, though challenging, is within reach. Commercial ADC systems have been reported with an ENOB of (roughly) 10-bits with sampling frequencies in excess of 100 MHz [3]. This suggests that the photonically assisted system presented here with

$N = 100$  would potentially yield a 10 Giga-sample per second ADC with the required ten bits of resolution. However other factors must also be considered which also limit the ENOB. As mentioned previously, the aperture uncertainty requirements are those of the high-speed ADC. The effective number of bits as a function of timing jitter is given by

$$\tau_a = \frac{1}{\sqrt{3} f_{\text{sample}}} 2^{-B} \quad (16)$$

from which we find that a 10-bit, 10 Gsps ADC requires an aperture uncertainty of roughly 65 fsec, another challenging requirement that can be met with a mode-locked (pulsed) laser clocking system, since solid-state clocks generally can provide uncertainties on the order of 1 ps [18].

### 3. EXPERIMENTAL RESULTS

The system shown in Figure (2) was constructed on an optical bench. A 1550 nm, 50 mw diode laser used as the optical source. The link was modulated using an 18 GHz - LiNbO<sub>3</sub> Mach-Zehnder modulator electrically driven with a 1 GHz tone burst. The RF modulated optical signal was injected into the recirculating delay loop via 3 dB coupler. A loop time delay of roughly 100 - nanoseconds was achieved using approximately 22 meters of single mode fiber with fine time delay adjustment ( $\pm 3$  nanoseconds) obtained from a variable delay line. Note also that the fundamental ring architecture with unity gain is essentially a laser. Since it lacks a frequency selective element the ring laser will act as a noise source and swamp any signal present in the loop unless lasing is prevented, and this is accomplished by using gates in both the input and ring circuits. The RF-modulated laser signal is gated into the loop for a specified time period and then disabled. Disabling the input gate prevents the laser signal from continuing to enter the ring once the RF signal has terminated. The ASE noise from the loop amplifier would again tend to stimulate lasing unless this effect is accounted for. This is accomplished by ensuring that the total loop delay is greater than the duration of the RF signal circulating in the loop. A second gate then essentially introduces significant loss in the loop and thus preventing lasing from occurring except for the time period required for the RF-modulated optical signal to pass through the loop gate. In this way, the loop gain is unity for a length of time which is less than the total loop delay so constructive interference cannot occur.

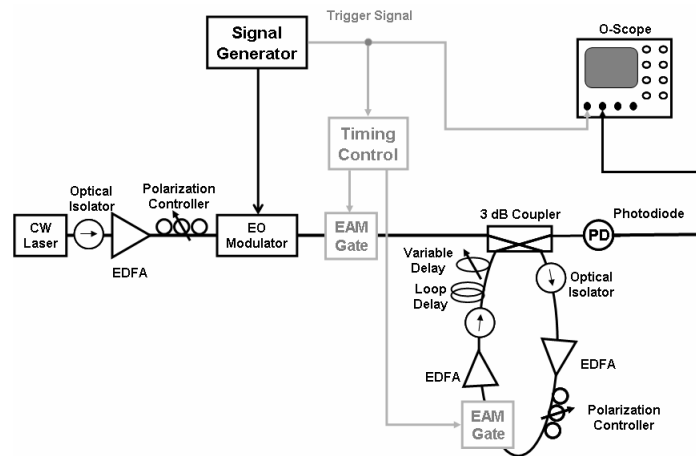


Figure 2: Experimental setup.

Once additional concern involves the gain dynamics of the loop's optical amplifier. With little or no light entering the amplifier when the loop gate is open, the turn-on time of the SOA when the light does enter will prevent the total required loop gain from being when needed. This effect is mitigated by using distributed amplification in the loop. For the experimental setup shown in Figure (2) two optical amplifiers were used in the loop which allowed for a lower gain in each amplifier and thus a faster turn-on time. Future implementation of the system would perhaps use either more amplifiers or else a continuously distributed amplification scheme.



The RF-modulated signal is gated in to the ring by allowing the modulated light Upon exiting the loop via the 3-dB coupler, the signal is directed to a 20 GHz PIN photodetector, and the resulting periodic signal is viewed on a high-speed oscilloscope. Also note that since the system was constructed with (connectorized) bulk optical components, this resulted in reduced SNR performance. Finally the time domain performance is shown in Figures (4) and (5).

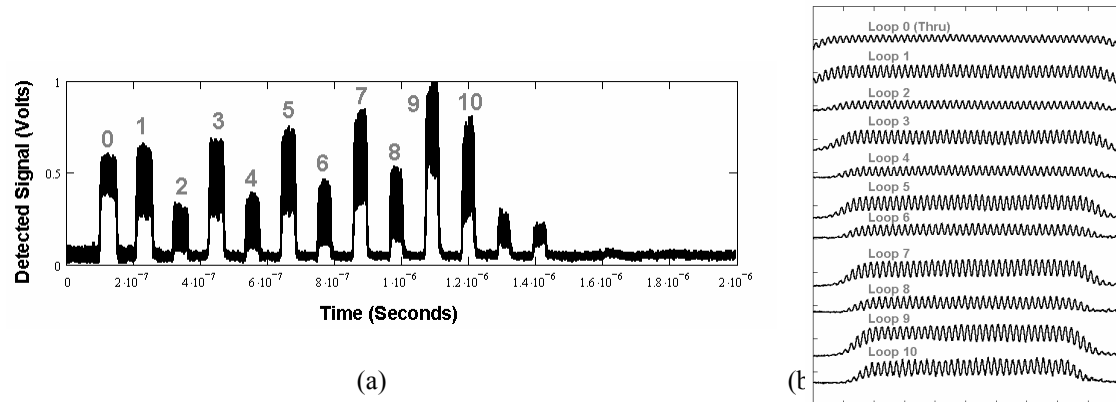


Figure 3: Measured output voltage for the thru signal and the first ten periods; (a) entire waveform, (b) details of pulses.

#### 4. CONCLUSIONS

This paper has presented a design for a simple yet effective way of implementing an ADC with the potential to achieve of both high-speed and high resolution. Preliminary data, obtained form a tabletop implementation, demonstrates, at least in-principle, the validity of the proposed ideas. A distinct advantage is that the ADC system can be realized by the appropriate modification of an existing fiber optic link. Furthermore, it was shown that the inclusion of the recirculating delay loop used to modify the link results in only a minimal reduction in the effective number of bits. Consequently the performance of the present ADC system improves as both fiber optic link technology and electronic ADC technology improves. Since these are the subject of great interest in the microwave photonics community, such improvements can be expected. This paper further quantified and provided accurate analytical estimates for critical parameters such as the ENOB, the overall noise figure, and the sampling rate.

The most severe restrictions on the ENOB arise from the required SFDR and aperture uncertainty. These restrictions are especially critical for broadband links that are generally thermal noise limited. Quantum limited detection is possible by using coherent detection but at the expense of a somewhat more complicated system and now with the concerns of added phase noise. The dynamic range of fiber optic links can be extended, in some cases significantly, by a variety of techniques. These include linearizing the output of the EO modulator by pre-distorting the input signal or by linearizing the modulator itself by utilizing multiple modulators to subtract out some of the nonlinear effects of a single Mach-Zehnder device. Though such approaches have proven effective, these techniques typically have sub-octave bandwidths and result in a more complicated system [16].

Since the noise figure of the recirculating delay loop represents a major source of SNR degradation, especially for a large number of circulations, it is important to reduce the laser (RIN) noise as must as possible. The RIN noise may be reduced to almost immeasurable levels by using a solid state laser source instead of the more common semiconductor or fiber laser.

Another inherent limitation with this approach is time required for digitization of a time packet  $T$  seconds long. The  $N$  – loop circulation needed to obtain all the samples, a processing time of approximately  $NT$  seconds is required. Because of the simplicity of the ADC structure, this drawback can be mitigated to some extent by using a time-multiplexed multiple ADC approach as is sometimes employed in the design of high-speed oscilloscopes. Other ways of addressing this issue involve the use of multi-wavelength systems and are currently under investigation. On the other hand, many high-speed applications such as radar only operate on a finite time portion of a signal so that the present system may be adequate.

A final concern, in fact one that exists for *any* high-speed ADC, is the timing accuracy of the signal samples. Though the present approach allows for the implementation of a “fast” ADC from a slower electronic ADC, the timing accuracy (jitter) for the slow ADC used in the implementation would likely not be insufficient for the high-speed operation. Adequate clock stability would require a separate timing unit for the ADC system. Since a suitable stable clock is an essential component for any ADC system, timing circuits employing stable mode-locked-lasers are being studied by several investigators [17, 18]. Timing stability concerns may also require that portions of the system, especially the recirculating loop, be placed in a temperature-controlled environment as is often done with high-speed test equipment. All of the above concerns discussed are currently under investigation and will be reported on at a later time.

## REFERENCES

1. H.F. Taylor, “An Optical Analog-to-Digital Converter,” *IEEE Journal of Quantum Electronics*, Vol. QE-15, pp. 210-216, 1979.
2. R.G Walker, I. Benian, and A.C, Carter, “Novel GaAs/AlGaAs Guided Wave Analogue/Digital Converter,” *Electronics Letters*, Vol. 25, pp. 1443-1444, Oct. 1989.
3. R.H. Walden, “Analog-to-digital converter survey and analysis,” *IEEE Journal of Selected Areas in Communications*, pp. 539-550, 1999.
4. T.R. Clark, Jr., and M.L. Dennis, “Toward a 100-Gsample/s Photonic A-D Converter” *IEEE Photonics Technology Letters*, Vol. 13, No. 3, March 2001, pp. 236-238.
5. M.J. Hayduk, R.J. Bussjager, and M.A. Getbehead, “Photonic Analog to Digital Conversion Techniques Using Semiconductor Saturable Absorbers,” *Proc. SPIE*, pp. 1-7, April, 2000.
6. M. Johansson, B. Lofving, S. Hard, L. Thylen, M. Mokhtare, U. Westergren, and C. Pala, “Study of an Ultrafast Analog-to-Digital Conversion Scheme Based on Diffractive Optics,” *Applied Optics*, **29**, no. 17, pp. 2881-2887, 10 June 2000.
7. E.N. Toughlian and H. Zmuda, “A Photonic Wide-Band Analog to Digital Converter,” International Topical Meeting on Microwave Photonics- MWP 2000, 11-13 September, Oxford, UK, pp. 248-250.
8. M.Y. Frankel, Jin U. Kang, and R.D. Esman, “High-performance photonic analogue-digital converter”, *Electronic Letters*, Vol. 33, pp 2096-2097, Dec. 1997.
9. Jin U. Kang, M.Y. Frankel, and R.D. Esman, “Highly parallel pulsed optoelectronic analog-digital converter”, *IEEE Photonics Technology Letters*, Vol. 10, pp. 1626-1628, Nov. 1998.
10. J.A. Bell. M.C. Hamilton, D.A. Leep, “A/D Conversion of Microwave Signals Using a Hybrid Optical/Electronic Technique,” *Proc. SPIE*, **1476**, pp 326-329, 1991.
11. P.E. Pace and D. Dtyer, “High-Resolution Encoding Process for an Integrated Optical Analog-to-Digital Converter,” *Optical Engineering*, **33**, no. 8, pp. 2638-2645, August 1994.
12. B. Jalali, F. Coppinger, A.S. Bushan, “Time-Stretch Preprocessing Overcomes ADC Limitations,” *Microwaves & RF*, pp. 57-66, March 1999.
13. E. Ackermann, “RF Fiber-Optic Links,” in Photonic Aspects of Modern Radar, H. Zmuda and E.N. Toughlian, editors, Boston: Artech House, 1994, pp.323-350.
14. W. Ng, R. Stephens, D. Persechini, and K.V. Reddy, “Ultra Low Jitter Mode-Locking of Er-Fiber Laser at 10 GHz and its Application to Photonic Analog-to-Digital Conversion,” International Topical Meeting on Microwave Photonics- MWP 2000, 11-13 September, Oxford, UK, pp. 251-254.

15. E.I Ackermann, "Broad-Band Linearization of a Mach-Zehnder Electrooptic Modulator," *IEEE Transaction on Microwave Theory and Techniques*, Vol. 47, No. 12, pp. 2271-2279, Dec. 1999.
16. U.V. Cummings and W. B. Bridges, "Bandwidth of Linearized Electrooptic Modulators," *IEEE Journal of Lightwave Technology*, Vol. 16, No. 4, pp. 1482-1490, Aug. 1998.